applied sciences

MDPI

Article

Does the monomer sequence influence the thermal behavior of poly(acrylonitrile-*co*-acrylamide)?

Roman V. Toms [1], Mikhail S. Balashov [1], Alexander Yu. Gervald [1], Nikolay I. Prokopov [1], Anna V. Plutalova [2], and Elena V. Chernikova [2]*

[1] MIREA—Russian Technological University, Institute of Fine Chemical Technologies named by M.V. Lomonosov, Moscow, 119571 Russia; toms.roman@gmail.com; diplomglue@gmail.com; gervald@bk.ru; prokopov@mirea.ru

[2] Lomonosov Moscow State University, Faculty of Chemistry, Leninskie Gory 1, bld. 3, 119991, Moscow, Russia; annaplutalova@gmail.com; chernikova_elena@mail.ru

* Correspondence: chernikova_elena@mail.ru

Abstract: In the present research, we have developed the controlled synthesis of acrylonitrile – acrylamide copolymers with desired monomer sequence distribution. By using dibenzyl trithiocarbonate and batch/semibatch polymerization, we have synthesized random, gradient and block gradient copolymers containing 3.4 – 10.2 mol. % of acrylamide to reveal if the monomer sequence can influence the thermal behavior of poly(acrylonitrile-*co*-acrylamide). Combination of differential scanning calorimetry and Fourier transform infrared spectroscopy allowed to find differences in thermal behavior of the copolymers in argon and air atmosphere. Intramolecular cyclization was the main process proceeding in argon atmosphere. The radical mechanism of cyclization was suppressed already at the molar part of AAM units in copolymer exceeding ~3 mol. % for random copolymer and ~6 mol. % for block gradient copolymer. The activation energy of ionic cyclization was equal to 89 ± 3 kJ·mol^{-1} and was not influenced by both copolymer composition and chain microstructure in contrast to the rate of cyclization. The latter was increased with the rise of acrylamide content and in the range block gradient < gradient < random structure. In air atmosphere, the oxidation reactions dominated over cyclization. The oxidation reactions were found to be less sensitive for copolymer composition and chain microstructure.

Keywords: polyacrylonitrile; precursor of carbon fibers; cyclization; thermo-oxidative stabilization.

1. Introduction

Copolymers of acrylonitrile (AN) are widely used for producing precursors of carbon fibers [1–6]. The final properties of the carbon fibers depend on the variety of factors including molecular characteristics of the polymer, the parameters of polymer molding, thermo-oxidative stabilization and carbonization [7]. The molecular characteristics of the polymer include copolymer composition, monomer sequence distribution, molecular weight (MW) and molecular weight distribution (MWD) of the polymer. Copolymer composition, MW and MWD can be varied in a wide range and are governed by polymerization conditions [8]. The monomer sequence distribution is set up by the monomer reactivity ratio and monomer feed ratio [9]. However, if the monomers have different activity in the copolymerization, i.e. they are consumed with different rates, then the monomer feed changes continuously throughout reaction resulting in the formation of macromolecules of various composition and monomer sequence distribution [8]. To overcome this problem, the monomer feed can be resembled constant by addition of each monomers with a given rate providing formation of macromolecules with similar composition during all the copolymerization. However, the synthesis of the copolymers with different monomer sequence distribution, but similar average composition in conditions of free

Citation: To be added by editorial staff during production.

Academic Editor: Firstname Lastname

Received: date
Revised: date
Accepted: date
Published: date

Copyright: © 2023 by the authors. Submitted for possible open access publication under the terms and conditions of the Creative Commons Attribution (CC BY) license (https://creativecommons.org/licenses/by/4.0/).

When monomers were?

please state briefly how compared to free radical polym.

radical copolymerization seems unlikely. At the same time, it becomes possible in conditions of reversible deactivation radical polymerization [10 – 12]. The prediction made in [13] for atom transfer radical copolymerization of AN and methyl acrylate was implemented further for copolymerization of AN and N-isopropyl acrylamide (NIPA) in conditions of reversible addition-fragmentation chain transfer (RAFT) polymerization [14]. The authors have demonstrated that the thermo-oxidative stabilization (TOS) of AN/NIPA copolymers was affected by monomer sequence distribution. As an example, the batch copolymerization resulted in the formation of the copolymer with the compositional drift along the backbone. Consequently, the cyclization reaction proceeded in the narrow temperature range with intensive heat release. While the slow addition of NIPA in the reaction led to the formation of the copolymer with uniform distribution of NIPA along the backbone, and the decrease of the intensity of heat release during cyclization and the increase of the breadth of the peak exotherm were observed. The reason for this effect comes from the ability of amide moiety to accelerate the cyclization reaction (Scheme 1):

This is out of context. Please quote prediction, its significance to this work and then reference.

In this work or in reference 13 or 14? Please consider clarifying these parts in the introduction.

→ Reference?

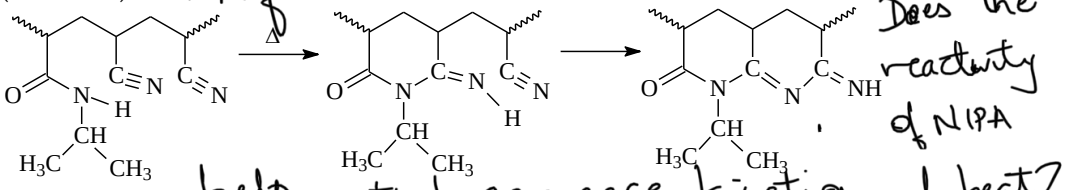

Does the reactivity of NIPA help control sequence, kinetics and heat?

Scheme 1. The proposed mechanism of the initiation of cyclization for the copolymer of AN and NIPA.

Is this proposed mechanism also the typically established mech.?

The similar approach was implemented in [15,16] for the copolymers of AN and acrylic acid (AA). Acrylic acid is able to accelerate the cyclization of nitrile groups similarly to amide-containing AN copolymer [17–19]. The batch, continuous and semi-continuous copolymerizations led to the formation of macromolecules with various drift of AA units along the backbone and to the drastic changes in thermal behavior of the copolymers.

Please see comments for highlighted sentences in the Reviewer comments file.

that can

Acrylamide (AAM) is another monomer being ~~able to~~ accelerate cyclization reaction. Its ability to accelerate cyclization of nitrile groups was described first in [20] on the example of the copolymers synthesized through copolymerization in water. To eliminate the composition heterogeneity of the copolymers, the synthesis was stopped at low monomer conversions. The nature of impact of AAM on the cyclization was proposed in [21] basing on the study of FTIR spectra of the similar AN and AAM copolymers subjected to thermal treatment under reduced pressure and in air. Cyclization can be observed even at 130 °C after induction period of 4 h, while at 160 °C induction period is about 1 h. After the induction period is completed, the intensities of the absorption bands corresponding to CN, CO, and NH groups fall drastically proving participation of AAM in cyclization. The proposed mechanism of cyclization initiated by AAM is rather complicated and involves several steps (Scheme 2) [20].

This would have altered other properties as well beyond thermal. right?

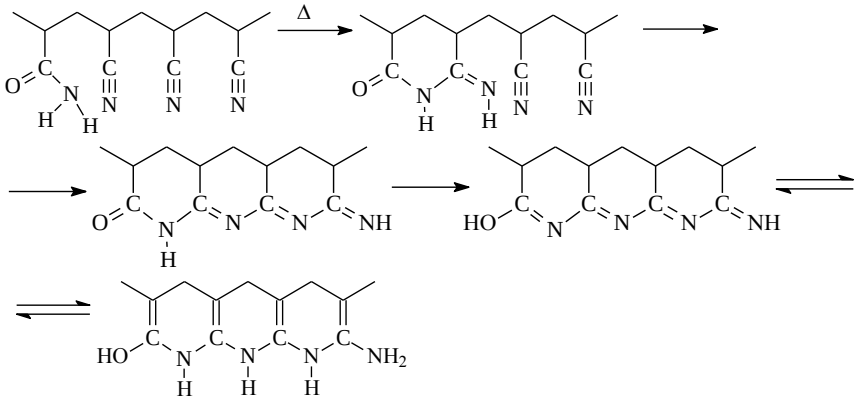

Scheme 2. The development of ladder structure in the copolymers of AN and AAM.

The influence of the copolymer composition on the cyclization reaction is rather interesting. Below 3 mol. % of AAM in the copolymer, cyclization proceeds slowly at both at 160 and 200 °C, while at AAM content above 5 mol. % the cyclization rate is higher and it does not depend on the copolymer composition indicating that the fraction of the available nitrile and amide groups that have reacted at the given time resembles constant [22]. Besides, the extent of the coloration of the copolymer films after the same time of treatment is inversely proportional to the concentration of AAM in the copolymer suggesting that the extent of conjugation decreases with the rise of AAM content in the copolymer. These observations have been gotten for the copolymers obtained by radical copolymerization in water with monomer reactivity ratios equal to r_{AN} = 1.5 and r_{AAM} = 0.3. In this case, the sequence length of AN units is 40 and 9 and AAM units 1 for the monomer feed with 2.5 and 10 mol. % of AAM. However, the simple calculations of the amount of AN units that can participates in cyclization reaction basing only on the monomer sequence distribution give the overrated results. However, if the stereochemistry (iso-/sindiotactic placements) is taken into account, then the experimental and theoretic values become close. In the latter model, amide group initiates the cyclization reaction if the neighboring nitrile group has isotactic placement, and the conjugation spreads over the backbone in the case of isotactic configuration of AN units (intramolecular cyclization) and transfers to another chain in the case of sindiotactic configuration of AN units (intermolecular cyclization).

In air atmosphere, the oxidation reactions take place along with cyclization. This conclusion is confirmed by FTIR analysis of the copolymers subjected to thermo-oxidative stabilization, which revealed the slow formation of pyridine structure and slow consumption of NH_2 groups [23]. The authors proposed that two processes compete with each other: intramolecular and intermolecular cyclization followed by oxidative reactions according to Scheme 3. It was supposed, that thermal treatment in air leads to the acceleration of dehydration reaction rather than cyclization. Besides, during the short induction period, amide groups reacts with neighboring nitrile groups forming cyclic structures. After reaching the critical concentration of these structures, the conjugation starts first through dehydration reaction followed by cyclization reaction.

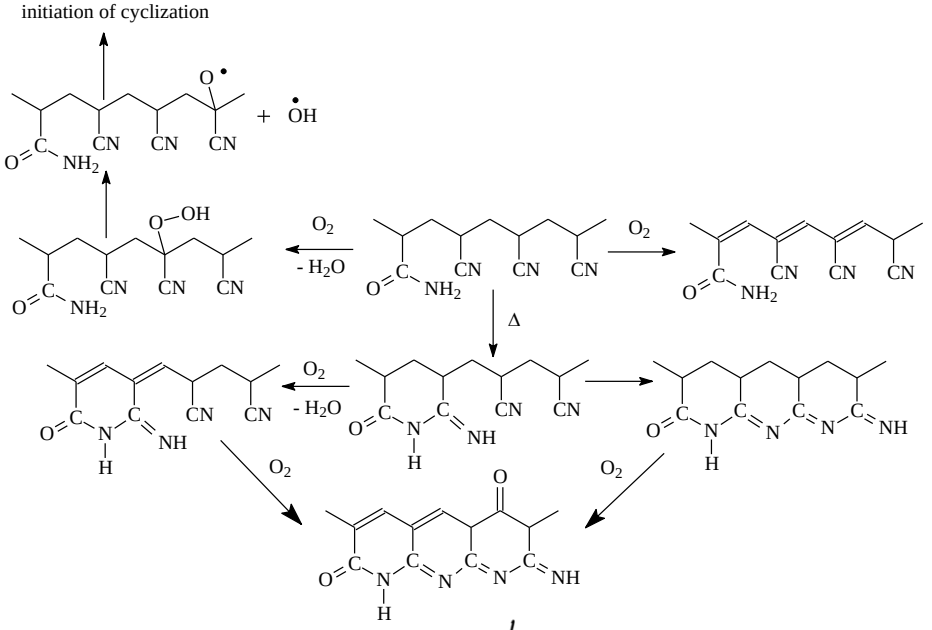

Scheme 3. The proposed mechanism of thermos-oxidative stabilization.

Obviously, that the change of the monomer activity will change the monomer sequence distribution and may affect the thermal behavior of AN and AAM copolymers. For example, in DMF or DMF–water mixtures the monomer reactivity ratios are $r_{AN} = 0.86$ and $r_{AAM} = 0.81$ [24]. The solvent polarity and polymer solubility give rise to a large variety of the monomer apparent reactivity ratios for AN and AAM [25]. Copolymerization in DMSO results in $r_{AN} = 0.65$ and $r_{AAM} = 1.68$ [26]. Although thermal behavior of various AN and AAM copolymers is described [20 – 23, 27–29], it seems impossible to establish the correlation between the monomer sequence distribution and the kinetics of cyclization of nitrile groups due to compositional heterogeneity of copolymers used in these studies.

In the present work we got on with the RAFT-based copolymers of AN and AAM formed in dimethylsulfoxide (DMSO) solution described in [30,31]. Along with control of MW and MWD, RAFT polymerization provides formation the copolymers with high compositional homogeneity. Combination of RAFT mechanism and controlled addition of AAM in the reaction provide the copolymer with tunable composition profile and allows finding the required correlation synthesis – copolymer microstructure – properties.

2. Materials and Methods

Acrylonitrile (99 %) supplied by "Acros" was distilled before use. Acrylamide (97%) from "Fluka" was recrystallized from chloroform. Azobisisobutyronitrile (AIBN) used as a radical initiator was recrystallized from ethanol and stored in a dark place at –3 °C. Dibenzyl trithiocarbonate ($C_6H_5CH_2$–S–C(=S)–S–$CH_2C_6H_5$, BTC) was synthesized and characterized according to the known procedure [32]. Dimethylsulfoxide (DMSO, 99%) and N,N-dimethylformamide (DMF, HPLC) supplied by "Fluka" was distilled under reduced pressure before use.

Polymerization was performed in a 100 mL three-neck flask equipped with an overhead device with an anchor-type stirrer. A solution containing the calculated amounts of AIBN and BTC dissolved in AN and DMSO was loaded in the flask. In the batch process, AAM was added also before the beginning of the polymerization. In the semi-batch process AAM was loaded in DMSO solution (1/1 wt) with a BYZ-810 syringe pump (Table 1). The detailed formulations are given in the Table S1, ESI. The flask was purged with argon (99.99 %) for 15 min, closed, and immersed in a bath heated to 80 °C. At a specified time, samples were taken for analysis. The total monomer conversion was determined gravimetrically by precipitating the polymer in the excess of deionized water.

Table 1. Formulations of the RAFT copolymerization of AN and AAM

Sample	Initial monomer feed, mol. %		Total f_{AAM} loaded in reaction, mol. %	Process	Addition of AAM
	f_{AN}	f_{AAM}			
1*	98	2	2	Batch	Together with AN
2*	95	5	5	Batch	Together with AN
3*	93	7	7	Batch	Together with AN
4**	93	7	7	Batch	Together with AN
5**	100	—	15.2	Semi-batch	AAM/DMSO mixture (1/1 wt) was introduced with the rate of 4 mL/h during 2 h from the reaction onset
6**	100	—	10	Semi-batch	AAM/DMSO mixture (1/1 wt) was introduced with the rate of 2 mL/h during 2.5 h from the reaction onset

7**	100	—	10	Semi-batch	AAM/DMSO mixture (1/1 wt) was introduced after 0.5 h from the reaction onset with the rate of 2 mL/h during 2.5 h

Note. * [AIBN] = [BTC] = 1 mmol/L, ** [AIBN] = [BTC] = 2 mmol/L

Samples for analysis by attenuated total reflection Fourier transform infrared (ATR FTIR) spectroscopy and differential scanning calorimetry (DSC) were prepared by dissolving copolymer in DMSO and cast onto glass substrate. The samples were then placed in the vacuum oven at 80 °C overnight. The resulted films were washed with water for 24 h to remove the residual DMSO, dried to the constant weight and separated from the surface. The films with average thickness of 20 – 50 μm were cut into pieces 20×20 mm and analyzed.

The degree sign can be inserted from symbols.

The average molecular weights and dispersity ($Đ_M = M_w/M_n$) were determined by the size exclusion chromatography (SEC). The SEC measurements were performed in DMF containing 0.1 wt % of LiBr at 50 °C with a flow rate of 1.0 mL/min using a chromatograph GPC-120 "PolymerLabs" equipped with refractive index and with two columns PLgel 5 μm MIXED B for MW range $5\times10^2 – 1\times10^7$. The SEC system was calibrated using narrow dispersed linear poly(methyl methacrylate) standards with MW ranging from 800 to 2×10^6 g mol^{-1}. A second-order polynomial was used to fit the $\log_{10}M$ versus retention time dependence. The molecular weights were recalculated for poly(acrylonitrile) using known coefficients of Mark–Houwink equation $K_1M_1^{\alpha1} = K_2M_2^{\alpha2}$, where $K = 39.4\times10^{-4}$, α=0.75 for PAN and $K = 17.7\times10^{-4}$, α=0.62 for PMMA [33].

FTIR spectroscopy in ATR mode (diamond crystal) was recorded using Spectrum Two FT-IR Spectrometer (PerkinElmer) in the range of 4000–400 cm^{-1}. For quantitative analysis of the composition of the films of the synthesized copolymers, the calibration curve was used (Figure S1). Calibration curve was obtained from the mixtures of the monomers of the known molar ratio. The ratio of the intensities, A of the characteristics bands assigned to ν_{CO} = 1690 cm^{-1} (AAM) and ν_{CN} = 2229 cm^{-1} (AN) was used [34]. The dependence of A_{CO}/A_{CN} on the molar ratio [AAM]/[AN] was linear. The copolymers of the known composition were used to confirm the validity of the calibration curves.

Differential scanning calorimetry was performed on a Netzsch DSC 204 (Netzsch, Germany) in the atmosphere of dry gas (air, argon) at flow rate of 100 mL·min^{-1} in the range of 30 – 500 °C and heating rate from 5 to 30 K·min^{-1} in air and 10 K·min^{-1} in argon. The activation energy of the reactions was determined by Kissinger method [35]:

How many mg was used for DSC from the 20×20 mm film?

$$-\frac{E_a}{R} = \frac{d\left[ln\left(\frac{\varphi}{T_p^2}\right)\right]}{d\left(\frac{1}{T_p}\right)} \quad (1)$$

where R – universal gas constant, T_p – peak temperature (K), φ – heating rate (K·min^{-1}).

FTIR spectra in ATR mode (diamond crystal) of the films subjected to thermal treating in argon at 200 °C and 225 °C and in air at 200 °C were recorded using Spectrum Two FT-IR Spectrometer (PerkinElmer) in the range of 4000–400 cm^{-1}. The proportion of the unreacted nitrile groups φ_{CN} [36] and stabilization index E_s were determined according to the equations [37]:

$$\varphi_{CN} = \frac{A_{2240\ cm^{-1}}}{A_{2240\ cm^{-1}} + fA_{1590\ cm^{-1}}} \quad (2)$$

$$E_s = \frac{A_{1590\ cm^{-1}}}{A_{2240\ cm^{-1}}} \quad (3)$$

where $A_{2240\ cm^{-1}}$ – intensity of the band assigned to –C≡N group, $A_{1590\ cm^{-1}}$ – intensity of the band assigned to –C=N– group, f – the ratio of the extinction equal to 0.29.

3. Results and Discussion

3.1. Copolymer synthesis

The copolymerization of AN with low amounts of AAM should proceed with similar rate as the homopolymerization of AN. Indeed, in the batch process the content of AAM in the monomer feed in the range of 2 – 7 mol. % has negligible effect on the copolymerization kinetics (Figure 1 a). Simultaneously, the kinetic plots are described by first-order kinetics (Figure 1b), which is typical for RAFT polymerization [38–41]. In semi-batch process, the total amount of AAM introduced into reaction is higher (10 – 15 mol. %, Table 1). However, due to the slow addition of AAM to the monomer mixture it has no visible effect on the copolymerization rate (Figure 1c). Similarly to the batch reaction, the copolymerization kinetics is first-order with respect to monomer concentration in the wide range of the polymerization time (Figure 1d).

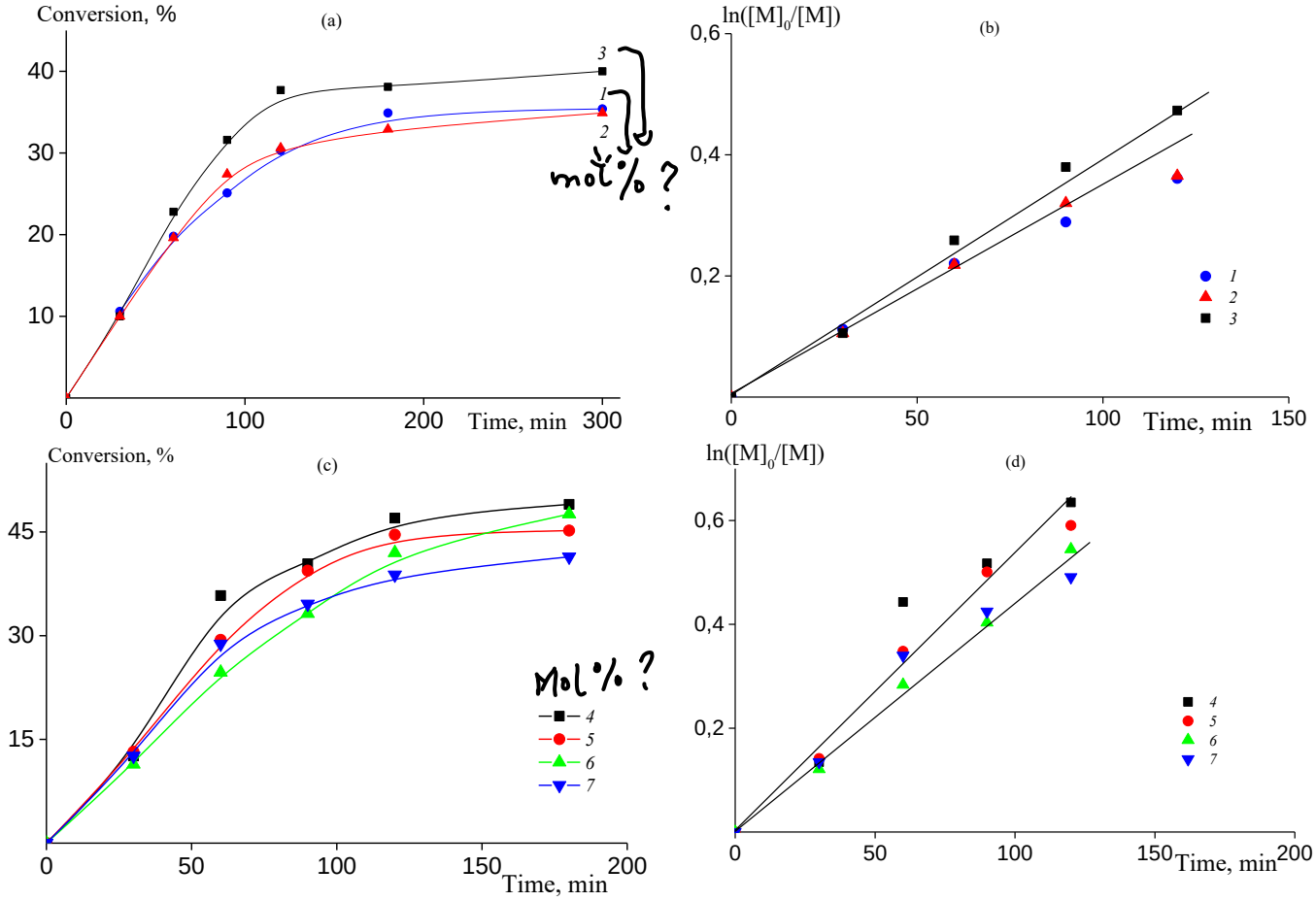

Figure 1. (**a, c**) Time – conversion dependences for AN – AAM copolymerization in 60 wt% DMSO at 80 °C, [AIBN] = [BTC] = 1 mmol/L (a) and [AIBN] = [BTC] = 2 mmol/L (c); (**b,d**) Corresponding semi-logarithmic dependences of the monomer concentration on the polymerization time. Numbering of the curves here and below corresponds to the numbering of the samples from Table 1.

The copolymer composition was studied by ATR FTIR spectroscopy. Figure 2 presents the dependences of the molar part of AAM units in the copolymers formed in batch and semi-batch processes on the monomer conversion. AAM is more active monomer than AN in solution polymerization in DMSO; the relative monomer activities are r_{AN} = 0.65 and r_{AAM} = 1.98 [26]. In batch copolymerization, the molar part of AAM units in the copolymer remains constant throughout reaction and the experimental values of copolymer composition (points) are in a good accordance with theoretical values (lines) calculated on the basis of r_{AN} and r_{AAM} values (Figure 2a). Semi-batch process gives an opportunity to control the introduction of AAM in the copolymer chain (Figure 2b, curves 2 – 4). The lower the rate of AAM addition to the reaction mixture, the lower the AAM content

in the copolymer. The average AAM molar fraction increases with the progress of the monomer conversion. In conditions of the free radical copolymerization, the change of the average copolymer composition is accompanied by the growth of the composition dispersity. For example, for imaginary experiment 7 conducted in the absence of BTC, when AAM was introduced after 0.5 h from the reaction onset with the rate of 2 mL/h during 2.5 h, the polymer formed at a period below 0.5 h should be pure PAN, while later a copolymer should form. In RAFT copolymerization the composition heterogeneity of macromolecules is replaced by the composition heterogeneity along macromolecule and all macromolecules have similar composition. For the real experiment 7, the polymer formed at a period below 0.5 h is also pure PAN, while later it is transferred to block-gradient due to chain-extension. Thus, combination of batch/semi-batch process with RAFT mechanism allows synthesis of the copolymers with various monomer sequence distributions.

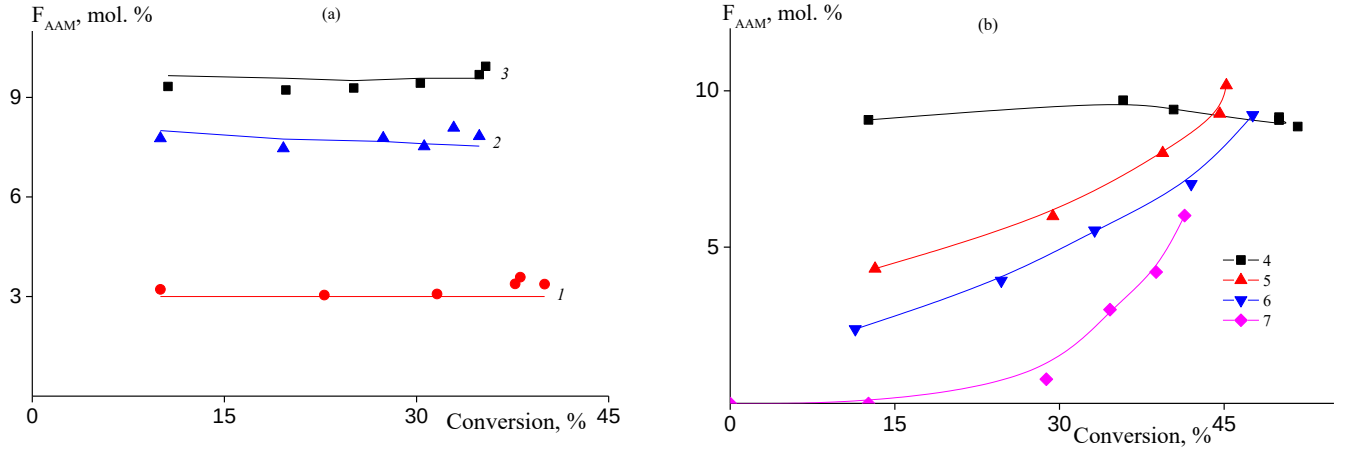

Figure 2. Dependences of the molar part of AAM in the copolymer on the monomer conversion in the copolymerization of AN and AAM at 80 °C. (**a**) [AIBN] = [BTC] = 1 mmol/L; (**b**) [AIBN] = [BTC] = 2 mmol/L.

Being active in cyclization reaction, the AAM unit distribution along the chain should affect the thermal behavior of AN/AAM copolymers. In batch process, triad composition at low monomer conversion and the instantaneous number-average sequence length of AN, $\langle N_{AN} \rangle_n$ and AAM, $\langle N_{AAM} \rangle_n$ can be evaluated on the assumption of the validity of terminal model kinetics from the equations (4) and (5) [9,42]:

$$F_{\text{AN-AN-AN}} = \left(1 - \frac{1}{1 + \frac{r_{AN} f_{AN}}{f_{AAM}}}\right)^2$$

$$F_{\text{AN-AN-AAM}} = F_{\text{AAM-AN-AN}} \frac{2}{1 + \frac{r_{AN} f_{AN}}{f_{AAM}}} \left(1 - \frac{1}{1 + \frac{r_{AN} f_{AN}}{f_{AAM}}}\right) \quad (4)$$

$$F_{\text{AAM-AN-AAM}} = \left(\frac{1}{1 + \frac{r_{AN} f_{AN}}{f_{AAM}}}\right)^2$$

$$F_{\text{AN-AAM-AN}} = \left(\frac{1}{1 + \frac{r_{AAM} f_{AAM}}{f_{AN}}}\right)^2$$

$$F_{\text{AAM-AAM-AAM}} = \left(1 - \frac{1}{1 + \frac{r_{\text{AAM}} f_{\text{AAM}}}{f_{\text{AN}}}}\right)^2$$

$$F_{\text{AN-AAM-AAM}} = F_{\text{AAM-AAM-AN}} \frac{2}{1 + \frac{r_{\text{AAM}} f_{\text{AAM}}}{f_{\text{AN}}}} \left(1 - \frac{1}{1 + \frac{r_{\text{AAM}} f_{\text{AAM}}}{f_{\text{AN}}}}\right)$$

$$\langle N_{AN} \rangle_n = \frac{1}{1 - \frac{r_{AN} f_{AN}}{f_{AN}(r_{AN} - 1) + 1}}$$

$$\langle N_{AAM} \rangle_n = \frac{1}{1 - \frac{r_{AAM} f_{AAM}}{f_{AAM}(r_{AAM} - 1) + 1}} \quad (5)$$

The accordance between experimental and theoretical values of copolymer composition confirms the validity of the terminal-model kinetics. The calculated values of triad composition and number-average sequence length of AN and AAM units are summarized in Table 2. Among AN centered triads, triads AN-AN-AN prevail, while among AAM-centered triads, triads AN-AAM-AN prevail in the triad composition of macromolecules. Homo-triads AAM-AAM-AAM and hetero-triads AAM-AN-AAM are unfavorable. The number-average sequence length of AN decreases with the rise of the AAM content in monomer feed, while the sequence length of AAM is about 1. Thus, the batch process suggests that AAM units are randomly distributed along macromolecules at $f_{AAM} \leq 7$.

Table 2. Triad composition and number-average sequence length of AN and AAM

f_{AAM}, mol. %	$F_{AN\text{-}AN\text{-}AN}$, mol. %	$F_{AN\text{-}AN\text{-}AAM} = F_{AAM\text{-}AN\text{-}AN}$, mol. %	$F_{AAM\text{-}AN\text{-}AAM}$, mol. %	$F_{AN\text{-}AAM\text{-}AN}$, mol. %	$F_{AAM\text{-}AAM\text{-}AN} = F_{AN\text{-}AAM\text{-}AAM}$, mol. %	$F_{AAM\text{-}AAM\text{-}AAM}$, mol. %	$\langle N_{AN} \rangle_n$	$\langle N_{AAM} \rangle_n$
7	40.2	9.3	0.5	37.9	11.3	0.8	9.6	1.1
5	42.8	6.9	0.3	41.0	8.5	0.5	13.3	1.1
2	47.0	2.96	0.04	46.2	3.7	0.1	32.8	1.0

Previously we have shown, that batch copolymerization of AN and AAM ($f_{AAM} \leq 10$) proceeded through RAFT mechanism in DMSO solution in the presence of BTC. Thus, it is expected that semi-batch process have the similar features. The SEC traces of the copolymers formed are given in ESI (Figure S2). Figure 3a demonstrates that the number-average molecular weight M_n of the copolymers increases linearly with the rise of the monomer conversion confirming RAFT mechanism of the process. Dispersion $Đ = M_w/M_n$ remains constant throughout copolymerization and remains lower (1.4 – 1.5) comparing to free radical process.

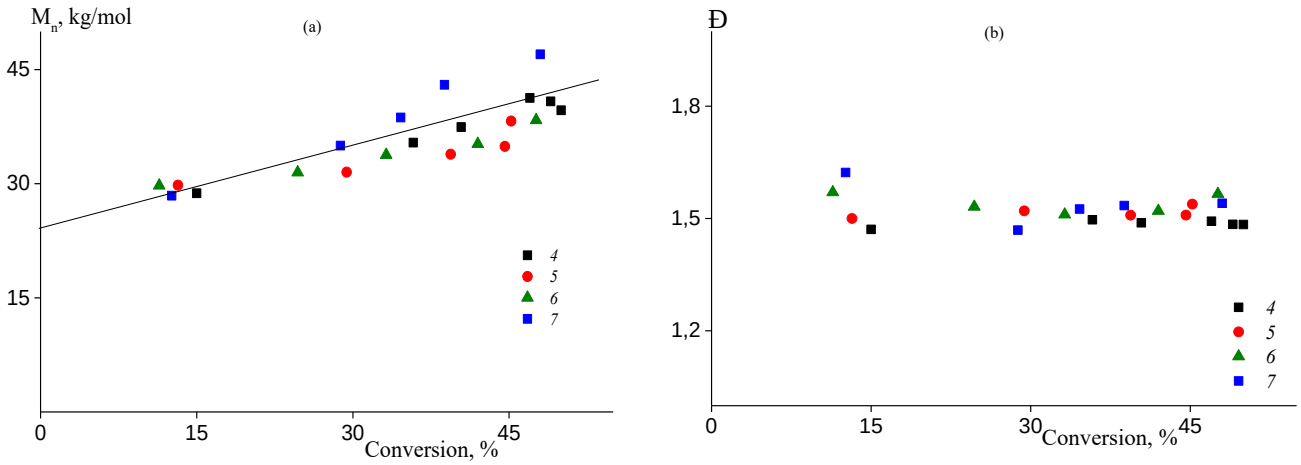

Figure 3. The dependences of the number-average molecular weight M_n **(a)** and dispersity Đ **(b)** on the monomer conversion of the copolymers formed in the RAFT copolymerization of AN and AAM at 80 °C and [AIBN] = [BTC] = 2 mmol/L.

Thus, RAFT copolymerization of AN and AAM allow the synthesis of the range of copolymers with random (experiments 1 – 4), gradient (experiments 5, 6) and block-gradient (experiment 7) structure. In contrast to monofunctional RAFT agents, BTC is bifunctional and has two leaving benzyl groups [43]. As a result, the macromolecule grows from the center to the tails according to the following reversible chain transfer reactions (Scheme 4).

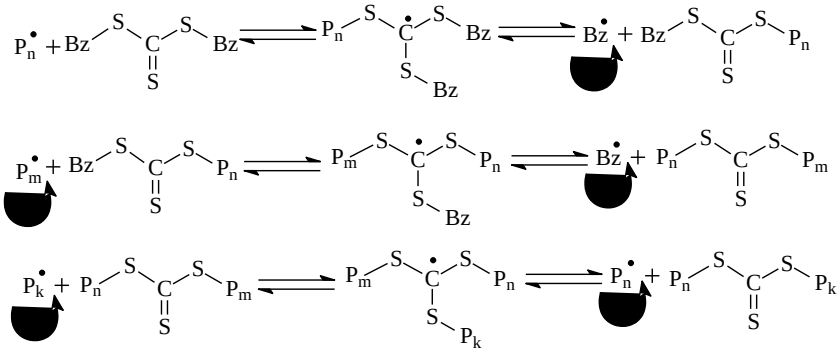

Scheme 4. The general scenario of the RAFT mechanism in the presence of BTC (Bz = benzyl).

Thus, the structure of random, gradient and block-gradient copolymers may be depicted as follows (Figure 4).

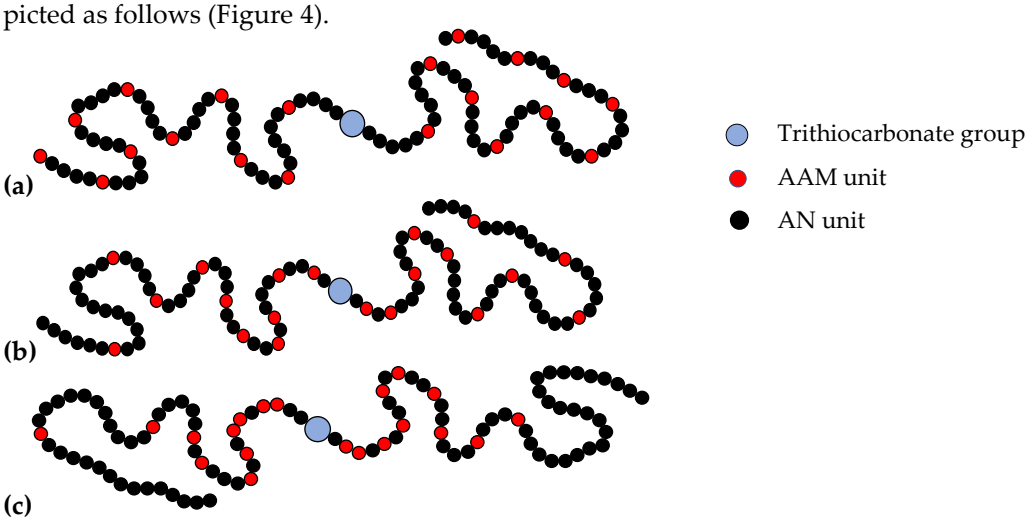

The results are interesting but ....

I wonder if the text can be revised to clarify that it is the cyclization reaction that is being investigated under inert and air thermal conditions using DSC.

Figure 4. Schematic presentation of the random (**a**), gradient (**b**) and block gradient (**c**) copolymers of AN and AAM obtained in the presence of BTC.

Below we shall consider the effect of the different monomer sequence distribution on the thermal behavior of the corresponding copolymers.

? Cyclization under thermal conditions ?

3.2. Thermal behavior of the copolymers ~~in the~~ inert ~~atmosphere~~: cyclization reaction

Thermal behavior of the copolymers was studied by DSC in the dynamic conditions. Figure 5a presents DSC thermograms of the copolymers registered in argon atmosphere at heating rate of 10 K/min; DSC curve of PAN is given for a comparison. Introduction of AAM affects the mechanism and the rate of the cyclization reaction. For random copolymers, at AAM content in the copolymer below ~ 9 mol. % both radical and ionic mechanism of cyclization are observed (curves 2 and 3). The low-temperature peak on the DSC thermogram is responsible for ionic mechanism of cyclization, while high-temperature peak is responsible for radical mechanism of cyclization. The ionic mechanism becomes predominant with further increase of AAM molar part in the copolymer (curve 4). The increase of AAM content in the copolymer leads to the rise of the heat flow corresponding to the ionic cyclization and to suppress of the heat flow corresponding to radical mechanism (Table 3). The chain unit distribution also affects the ratio of the radical and ionic mechanisms (curves 5 – 7). For block gradient copolymer (curve 7), the central block of gradient copolymer is attached to the terminal blocks of PAN resulting in the separate manifest of ionic and radical mechanisms. In gradient copolymers (samples 5 and 6), the AAM content increases from the center of the macromolecule to its tails. In this case, the radical cyclization is suppressed practically. The DSC data are summarized in Table 3.

It is NOT the thermal behavior of the final polymer to reveal physical structure properties.

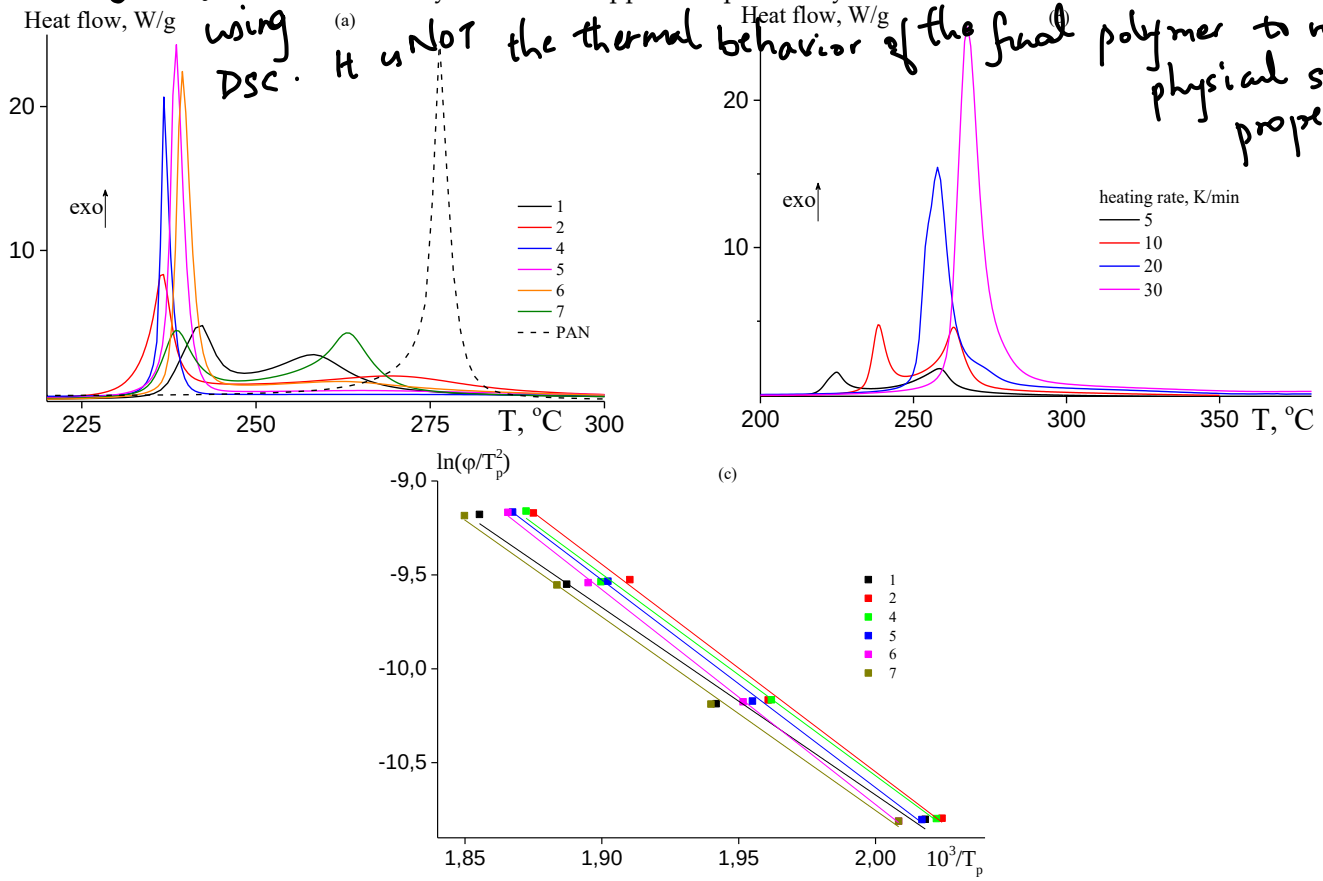

Figure 5. (**a**) DCS thermograms of the copolymers 1, 2, 4 – 7 and PAN registered in argon at heating rate 10 K·min^{-1}; (**b**) DCS thermograms of samples 7 registered in argon at different heating rates (5 – 30 K·min^{-1}); (**c**) dependence of ln(φ/T_P^2) on 1/T_P for the copolymers of AN and AAM 1, 2, 4 – 7.

Table 3. DSC data for the copolymers of AN and AAM registered in argon atmosphere.

Sample	F_{AAM}, mol.%	AAM distribution	T_p, °C *	Heat flow at T_p, J·g^{-1} *	$-\Delta H$, J·g^{-1} *	E_a, kJ·mol^{-1}
PAN	0	-	276	25	493	113±8
1	3.4	Random	242, 258	4.8, 2.8	460	83±5
2	7.8	Random	236, 269	8.3, 1.3	638	92±3
4	8.8	Random	236	20.7	429	89±3
5	10.2	Gradient	238	24.3	609	92±2
6	9.2	Gradient	239, 262	22.4, 0.9	662	95±2
7	6.0	Block-gradient	239, 263	4.4, 4.3	656	86±3

* Detected at a heating rate 10 K/min.

It is interesting to evaluate the activation energy as a function of monomer unit sequence. Figure 5b presents the DCS thermograms of sample 7 registered at different heating rates. The increase of heating rate leads to shift of the thermogram to the region of high temperature and to increase of their area. It is notable that the shape of thermogram changes. At low heating rate (5 K·min^{-1}) two peaks are observed. The low-temperature peak shifts faster with the rise of the heating rate in contrast to high-temperature peak. As a result, only one low-temperature peak is observed at high heating rate (20 K·min^{-1}), which make impossible to determine the activation energy of the radical cyclization and allow estimation of ionic cyclization only. The corresponding thermograms for other copolymers are presented in ESI (Figure S3). To calculate the activation energy, the dependence of $\ln(\varphi/T_p^2)$ on T_p^{-1} was plotted (Figure 5c). According to equation (1), the activation energy of ionic cyclization was determined from the slope of the linear dependence. As is seen from Table 3, the activation energy of radical cyclization (determined for pure PAN) is about 20 kJ·mol^{-1} higher than that of ionic cyclization initiated by amide group. The calculated value of ionic cyclization (89 ± 3 kJ·mol^{-1}) is close to determined before for AN – AAM – alkyl acrylate systems [31]. In contrast to previous reports [44], the activation energy of ionic cyclization is not influenced by AAM content in the copolymer. Also, it is not influenced by the monomer sequence distribution. It may be supposed that for the investigated systems the development of the conjugation starts after achieving certain amount of the cycles formed through reaction of amide and nitrile groups (Scheme 1).

The analysis of the chemical changes that occur during cyclization reaction may give deeper understanding of the formation of ladder structure in AN and AAM copolymers depending on their microstructure. Figure 6 shows the FTIR spectra of random (a), gradient (b), and block-gradient (c) copolymers registered after isothermal heating of the samples at 200 °C at various time.

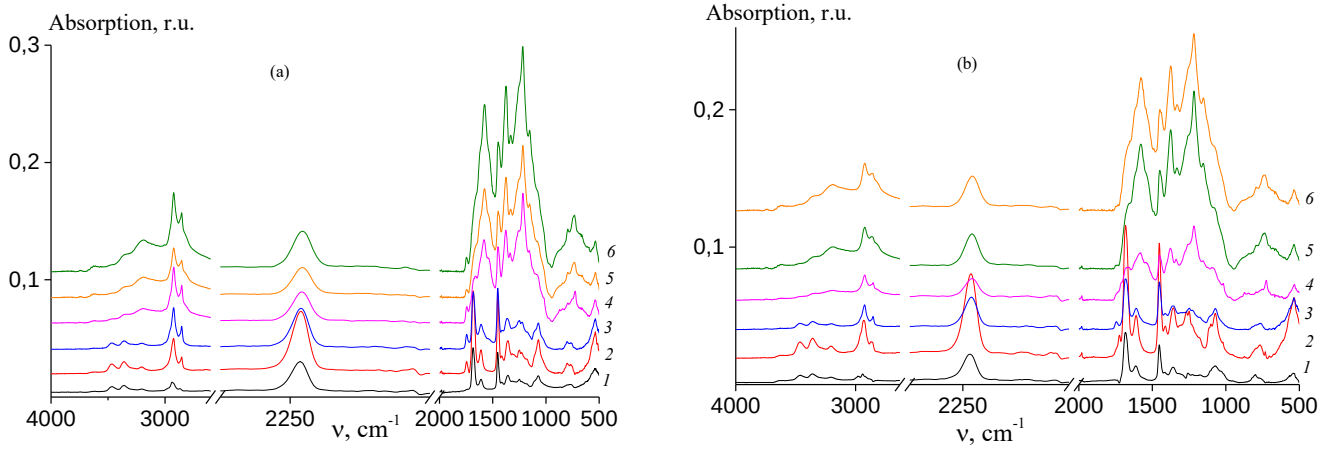

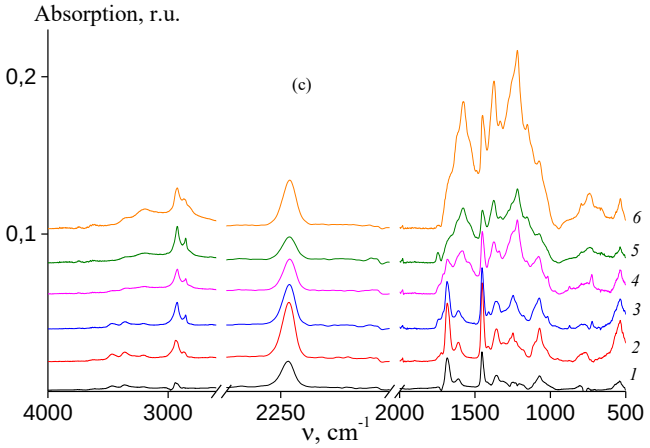

Figure 6. FTIR spectra of AN and AAM copolymers subjected to thermal treatment in Ar atmosphere at 200 °C for 0 (1), 5 (2), 10 (3) 20 (4), 60 (5), and 120 min (6): (**a**) random copolymer 2 (F_{AAM} = 7.8 mol. %); (**b**) gradient copolymer 6 (F_{AAM} = 9.2 mol. %); (**c**) block-gradient copolymer 7 (F_{AAM} = 6.0 mol. %).

In the spectra of non-treated copolymers (curves 1) the characteristic absorbance bands of AN and AAM units are observed. The following bands are observed: stretching vibrations of CN groups at 2244 cm^{-1}, stretching vibrations of CH groups at 2990 – 2920 cm^{-1}, bending vibrations of CH_2 groups are at 1453 and 1360 cm^{-1}, mixed vibrations at 1257 and 1073 cm^{-1}, stretching vibrations of C=O at 1685 and 1613 cm^{-1}, and N–H stretching vibrations at 3462 and 3357 cm^{-1} [21].

Upon heating at 200 °C, the chemical structure of the copolymers changes and the new bands appear in the spectra and/or the intensity of the existing bands changes (curves 2 – 6). The reduction of nitrile stretching absorbance at 2244 cm^{-1} and carbonyl stretching absorbance at 1685 cm^{-1} is observed as compared with intensity of vibrations of CH and CH_2 groups (2990 – 2920, 1453 cm^{-1}). The similar trend is observed for N–H stretching vibrations at 3462 and 3357 cm^{-1}. A new low intense band appears at 1745 cm^{-1} and its intensity decreases upon further heating. The bands at 3190, 1581, 1540, 1370, 1247, 1220, 1150, 795, 740, and 660 cm^{-1} appear and their intensity increases with the rise of duration of heating. These bands, except bands at 1745 and 1220 cm^{-1}, belong to pyridone type structure formed in pure PAN. The absence of the absorbance at 1700 cm^{-1} indicates the existence of amide–iminol tautomerism. It is important to note that the band at 2244 cm^{-1} resembles its shape and no traces of the band 2200 cm^{-1} is observed; the latter corresponds to nitrile group conjugated to the olefinic group. The absence of the bands at 810 and 960 cm^{-1} referred to CH bending vibrations in olefins along with the absence of the band at 2200 cm^{-1} confirms that no dehydration takes place. Similar trends are observed for other studied copolymers and for all the samples upon the heating at 250 °C (Figures S4, S5, ESI). All these changes are typical for cyclization reaction of AN and AAm copolymers [20,21]. Thus, the copolymer composition and copolymer microstructure has no impact on the chemical changes of the copolymers during cyclization. However, the rate of formation of ladder structure depends on the factors mentioned above (Figure 7).

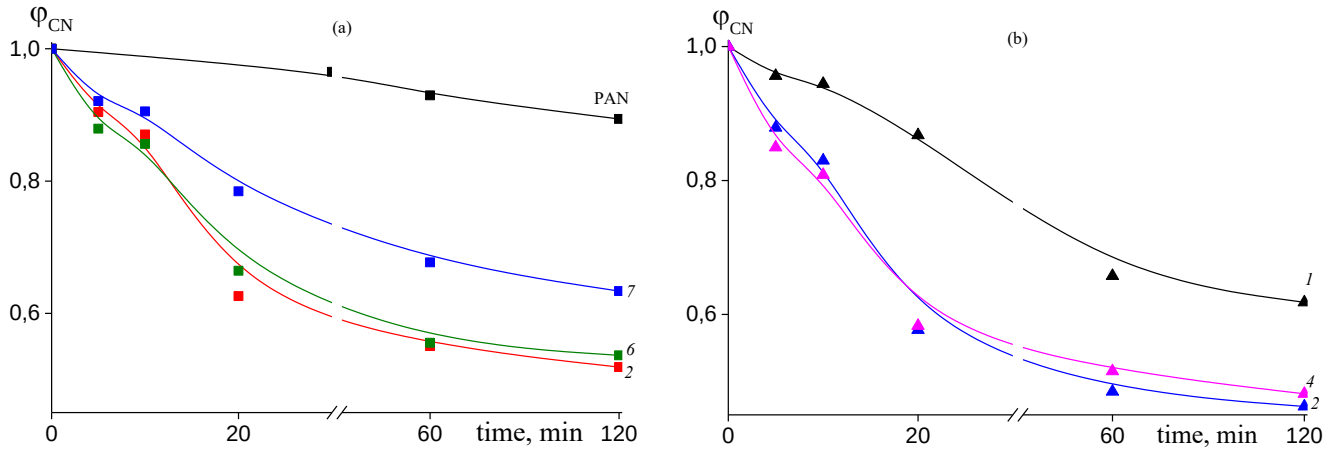

Figure 7. Dependence of the proportion of the unreacted nitrile groups φ_{CN} on the time of heat treatment at 200 °C for: (**a**) PAN, random copolymer 2 (F_{AAM} = 7.8 mol. %) (2), gradient copolymer 6 (F_{AAM} = 9.2 mol. %) (6), and block-gradient copolymer 7 (F_{AAM} = 6.0 mol. %) (7); (**b**) random copolymer 1 (F_{AAM} = 3.4 mol. %) (1), random copolymer 2 (F_{AAM} = 8.8 mol. %) (2), and gradient copolymer 4 (F_{AAM} = 10.2 mol. %) (4).

Addition of AAM in PAN structure results in noticeable acceleration of cyclization reaction. The conversion of nitrile groups increases with the rise of content of AAM in the copolymer (Figure 7). However, if we compare copolymers of various microstructures, we can see that conversion of nitrile groups decreases in the following order of copolymers: random > gradient > block-gradient. Another way to the quantitative analysis of the kinetics of the cyclization reaction is the analysis of the dependence of the stabilization index E_s on the time of heat treatment, which gives information about development of the ladder structure. Figure 8 presents corresponding dependences for copolymers obtained at 200 (a) and 250 °C (b). The higher the E_s value, the more developed the ladder structure. At 200 °C both the copolymer composition and microstructure affect the E_s (Figure 8a). The dependences have S-shape. The rise of AAM content in the copolymer leads to the growth of E_s value. Similar trend is observed: the E_s value decreases from block-gradient to gradient to random copolymer. The increase of the temperature up to 250 °C resembles the difference between PAN and copolymers (Figure 8b). However, the impact of the copolymer composition and microstructure becomes less pronounced due to higher cyclization rate. The influence of the copolymer composition on the cyclization rate is clear and comes from the increase of the initiation rate (Scheme 1). The influence of chain microstructure is less evident. From our point of view, the gradient structure may increase the probability of formation of AAM centered triads (AAM-AAM-AAM, AN-AAM-AAM and AN-AAM-AN). As a result, the less AAM units participates in the initiation of ionic cyclization of nitrile groups resulting in the decrease of the cyclization reaction. The rise of the temperature leads to the increase of the initiation rate and shortens its duration. Thus, it becomes difficult to observe the influence of the copolymer composition and microstructure on the cyclization rate.

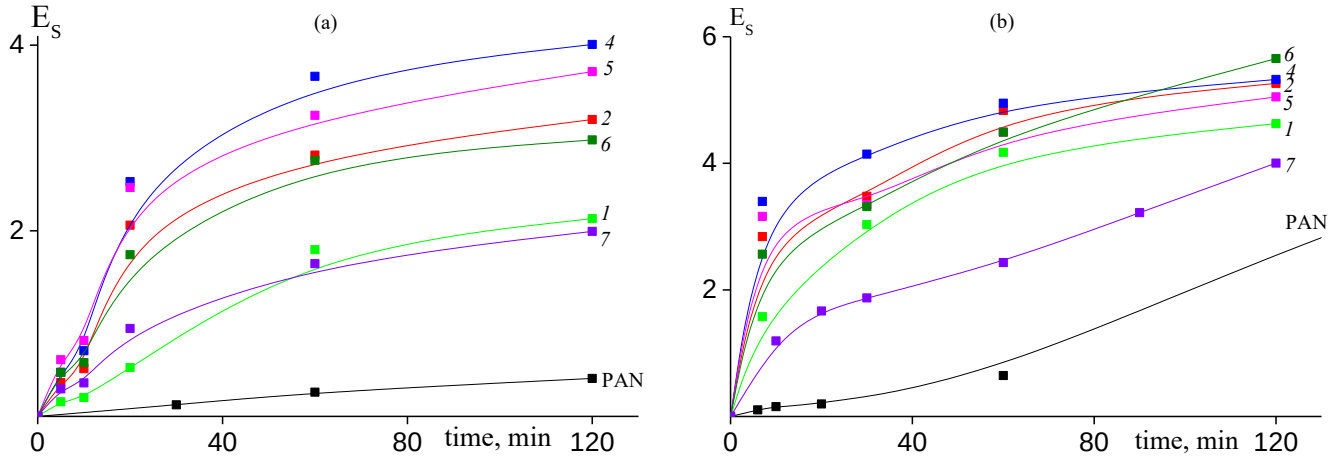

Figure 8. Dependence of the stabilization index E_s on the time of heat treatment at 200 °C (**a**) and 225 °C (**b**) for PAN and AN/AAM copolymers (2 – 7). Numeration of the curves corresponds to the numeration of the samples in Table 1.

3.3. Thermal behavior of the copolymers in air

The similar experiments in dynamic and isothermal conditions have been conducted in air atmospehere. Figure 9 presents DSC thermograms of random copolymers with various compositions (a) and copolymers with various microstructures (b).

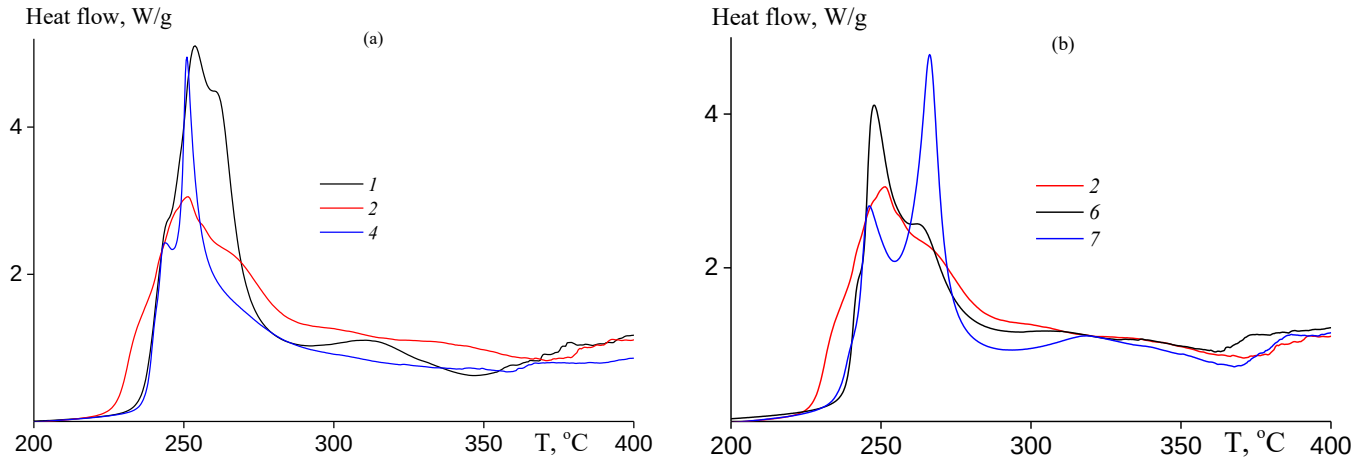

Figure 9. DCS thermograms registered in air at heating rate 10 K·min^{-1} of (**a**) the random copolymers 1, 2, 4; (**b**) random 2, gradient 6 and block gradient copolymer 7.

The exo-effect can be observed at lower temperatures as compared with experiment in argon atmosphere and its intensity at the temperature of the maximum of heat release is several times less (see Figs. 5a, 5b); the multiple peaks corresponding to various chemical processes are observed. Both chemical composition and chain microstructure affect the shape of the thermogram, i.e. the contribution of the chemical reactions proceeding upon thermal treatment in air atmosphere (Table 4). The increase of the number of the chemical reactions causes the rise of the value of the enthalpy of the process.

Table 4. DSC data for the copolymers of AN and AAM registered in air.

Sample	F_{AAM}, mol.%	$T_{on\text{-}set}$, °C	T_p, °C	–ΔH, J·g^{-1}
1	3.4	236	243, 254, 262, 311	895
2	7.8	228	233, 251, 266, 302, 366	855
4	8.8	236	244, 251	720
5	10.2	236	242, 254, 267, 308, 340	740

6	9.2	238	241, 248, 264, 315, 340	770
7	6.0	238	240, 246, 266, 330	920

Upon heating at 200 ° in air atmosphere, the chemical structure of the copolymers changes. These changes can be followed by FTIR spectroscopy (Figure 10). No visible qualitative differences are observes during transformation of FTIR spectra of random (a), gradient (b) and block gradient (c) copolymers. However, the differences are observed by comparison Figures 6 and 10 conforming to changes in the chemical structure of the copolymers after heating during the same period in argon (Figure 6) and in air (Figure 10). In argon, the pyridone type structure become dominant after 30 min. In air, the number of new bands is less, and the most noticeable changes are due to the band at 1590 cm^{-1} that stands out above the band of initial amide group at 1680 cm^{-1} only after 90 min. Simultaneously, the bands at 816 and 956 cm^{-1} (CH bending vibrations in olefins) become visible upon treatment in air and are absent in argon. The reduction of intensity of nitrile group at 2244 cm^{-1} and NH in amide group at 3480 cm^{-1} occurs slowly.

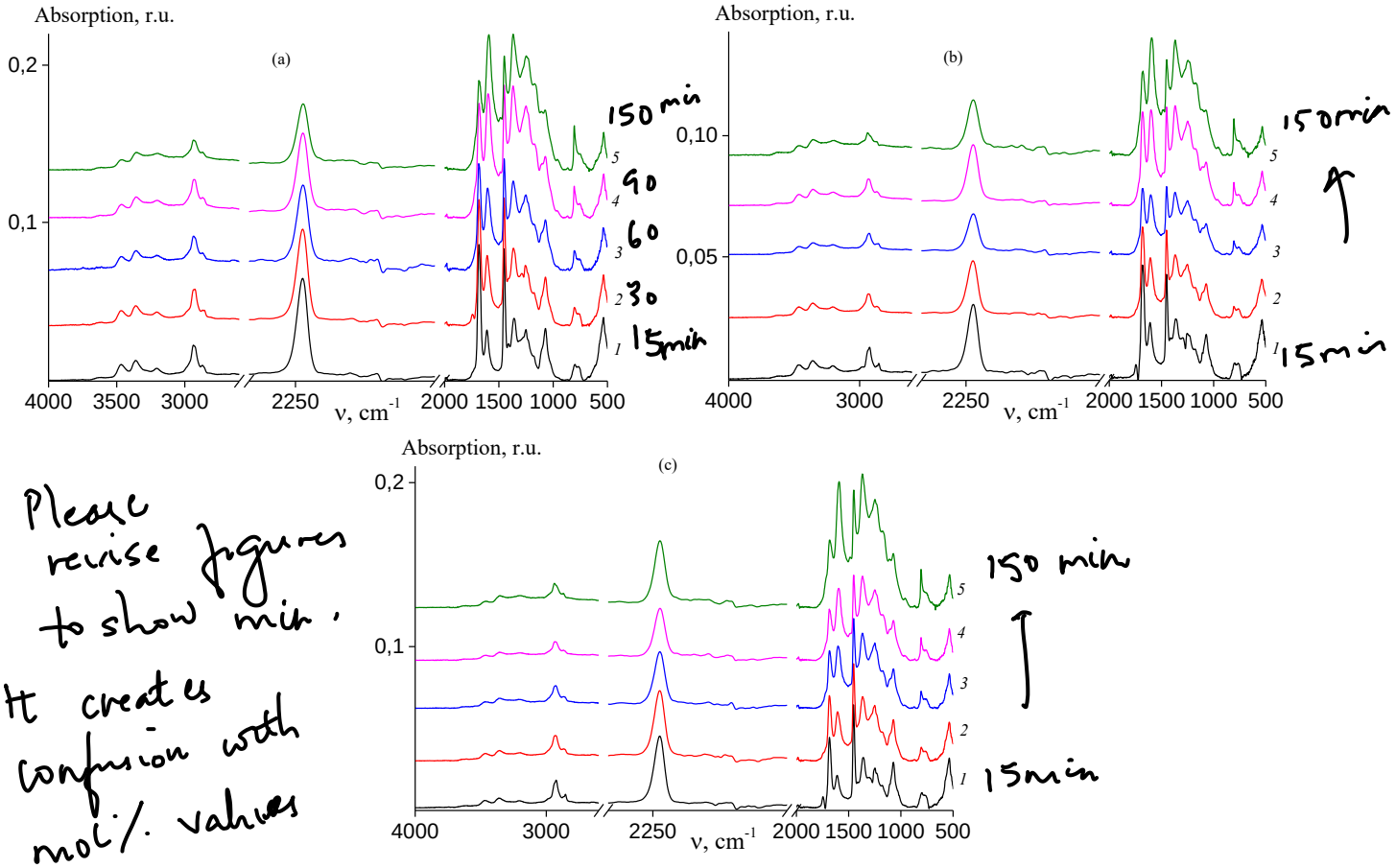

Please revise figures to show min. It creates confusion with mol/. values used for figures above.

Figure 10. FTIR spectra of AN and AAM copolymers subjected to thermal treatment in air at 200 °C for 15 (1), 30 (2), 60 (3), 90 (4), and 150 min (6): (**a**) random copolymer 2 (F_{AAM} = 7.8 mol. %); (**b**) gradient copolymer 6 (F_{AAM} = 9.2 mol. %); (**c**) block-gradient copolymer 7 (F_{AAM} = 6.0 mol. %).

The lower conversion of nitrile groups is confirmed by Figure 11a. The rate of intramolecular cyclization reaction in air atmosphere is smaller as compared to experiment in argon atmosphere (Figure 7). Thus, cyclization is not a dominant reaction upon heating the copolymers at 200 °C in air. Moreover, it is less sensitive to the amount of amide groups in the copolymer, except the sample 1, containing least value of AAM units (3.4 mol. %), and to the copolymer microstructure. As a consequence, the stabilization index reflecting the development of the ladder structure is relatively low.

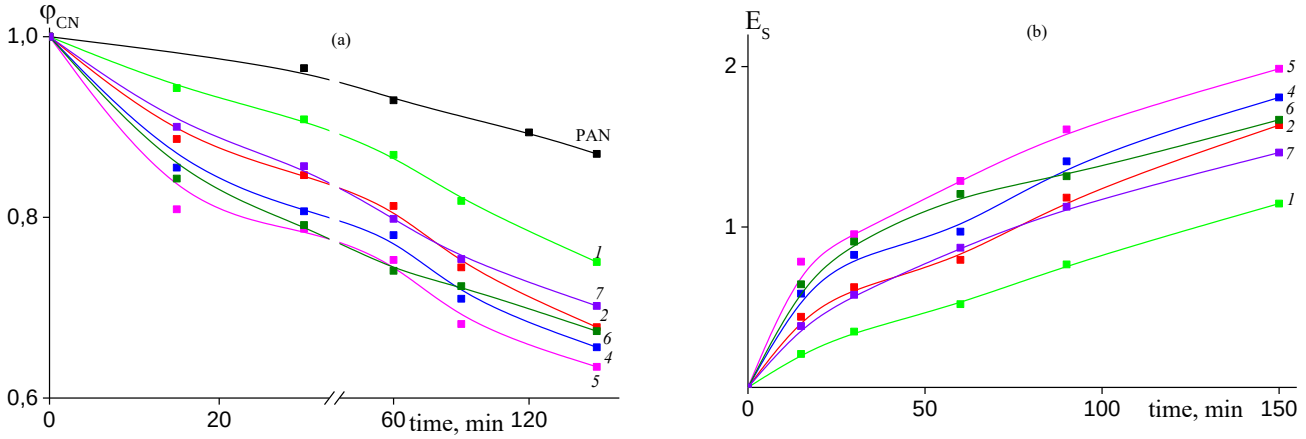

Figure 11. Dependence of the proportion of the unreacted nitrile groups φ_{CN} (**a**) and stabilization index E_s (**b**) on the time of heat treatment at 200 °C for PAN and AN/AAM copolymers (2 – 7). Numeration of the curves corresponds to the numeration of the samples in Table 1.

Summarizing FTIR data, it may be proposed that in oxidative conditions (upon heating in air), the formation of the conjugated C=C bonds occurs faster than of the C=N bonds for AN/AAM copolymers (Scheme 5). As a result, the ladder structure develops slowly at least at 200 °C. The important role of oxidation reaction is in accordance with [23].

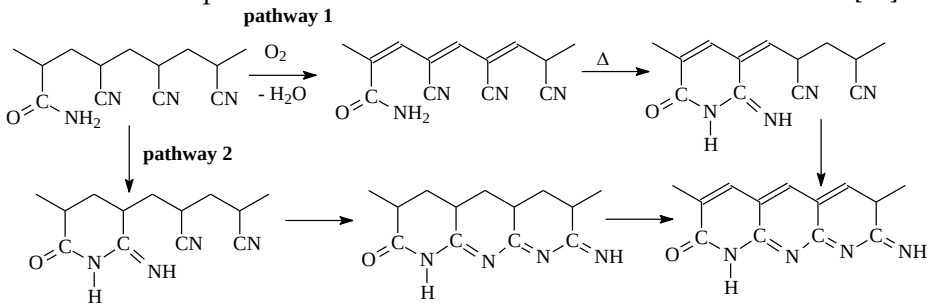

Scheme 5. The proposed mechanism of thermos-oxidative stabilization for the copolymers of AN and AAM.

4. Conclusions

In the present study we have synthesized a number of copolymers of AN and AAM with desired MW, narrow MWD and various monomer sequences (random, gradient and block gradient). These RAFT-based copolymers were used to clarify the influence of chain microstructure on the thermal behavior of the copolymers in inert and air atmosphere.

Please see comments above

We have demonstrated that cyclization reaction dominated in Ar atmosphere. The ionic mechanism of cyclization prevailed over radical one if the molar part of AAM units in copolymer exceeded ~3 mol. % for random copolymer and ~6 mol.% for block gradient copolymer. The activation energy of ionic cyclization was not influenced by both copolymer composition and chain microstructure.

On the contrary, the oxidation reactions dominated in air atmosphere. In this case, the formation of conjugated C=C bonds developed along with conjugated C=N bonds resulting in the lower values of the conversion of nitrile groups. The oxidative reactions were found to be less sensitive for copolymer composition and chain microstructure.

Thus, it may be proposed that the low content of AAM units (~ 3 mol. %) randomly distributed along the chain is enough to perform successful thermo-oxidative stabilization of AN copolymer.

Supplementary Materials: The following supporting information can be downloaded at: www.mdpi.com/xxx/s1, Figure S1: Calibration curve for determination copolymer composition;

Figure S2: SEC traces of the copolymers formed in the experiments 4 – 7 (Table 1) at various conversions; Figure S3: DCS thermograms of samples 1, 2, 4 – 6 registered in argon at different heating rates; Figure S4: FTIR spectra of AN and AAM copolymers subjected to thermal treatment in Ar atmosphere at 200 °C for 0 (1), 5 (2), 10 (3) 20 (4), 60 (5), and 120 min (6); Figure S5: FTIR spectra of AN and AAM copolymers subjected to thermal treatment in Ar atmosphere at 225 °C for 0 (1), 7 (2), 30 (3) 60 (4), and 120 min (5); Table S1: Formulations of the RAFT copolymerization of AN and AAM.

Author Contributions: Conceptualization, E.C.; methodology, R.T, A.G.; investigation, R.T., M.B., A.P.; writing— original draft - E.C., writing – editing – N.P. All authors have read and agreed to the published version of the manuscript.

Funding: This research received no external funding.

Data Availability Statement: Not applicable.

Conflicts of Interest: The authors declare no conflict of interest.

References

1. Frank, E.; Hermanutz, F.; Buchmeiser, M.R. Carbon Fibers: Precursors, Manufacturing, and Properties. *Macromol. Mater. Eng.* **2012**, *297*, 493–501.
2. Frank, E.; Steudle, L.M.; Ingildeev, D.; Spörl, D.-C.J.M.; Buchmeiser, M.R. Carbon Fibers: Precursor Systems, Processing, Structure, and Properties. *Angew. Chem. Int. Ed.* **2014**, *53*, 5262–5298.
3. Huang, X. Fabrication and Properties of Carbon Fibers. *Materials* **2009**, *2*, 2369–2403.
4. Kaur, J.; Millington, K.; Smith, S. Producing high-quality precursor polymer and fibers to achieve theoretical strength in carbon fibers: A review. *J. Appl. Polym. Sci.* **2016**, *133*, 43963.
5. Khayyam, H.; Jazar, R.N.; Nunna, S.; Golkarnarenji, G.; Badii, K.; Fakhrhoseini, S.M.; Kumar, S.; Naebe, M. PAN precursor fabrication, applications and thermal stabilization process in carbon fiber production: Experimental and mathematical modelling. *Prog. Mater. Sci.* **2019**, *107*, 100575.
6. Newcomb, B.A. Processing, structure, and properties of carbon fibers. *Compos. Part A Appl. Sci. Manuf.* **2016**, *91*, 262–282.
7. Morgan, P. (Ed.) *Carbon Fibers and Their Composites*; Taylor and Francis: New York, NY, USA, 2005; pp.185 - 259.
8. Odian, G. *Principles of Polymerization*, 4th ed.; Wiley-Interscience: Hoboken, NJ, USA, 2004; pp. 198 – 506.
9. Tirell, D.A. Copolymer Composition. In *Comprehensive Polymer Science and Supplements*. Allen, G., Bevington, J.C., Eds.; Elsevier: Amsterdam, Netherlands; 1989, Vol. 3, pp. 195 – 206.
10. Chernikova, E.V.; Mineeva, K.O. Reversible Deactivation Radical Copolymerization: Synthesis of Copolymers with Controlled Unit Sequence. *Polym. Sci., Ser. B.*, **2022**,
11. Borisova, O.; Billon, L.; Zaremski, M.; Grassl, B.; Bakaeva, Z.; Lapp, A.; Stepanek, P.; Borisov, O. Synthesis and pH- and salinity-controlled self-assembly of novel amphiphilic block-gradient copolymers of styrene and acrylic acid. *Soft Matter.* **2012**, *8* (29), 7649 – 7659.
12. Kozhunova, E. Yu.; Plutalova, A. V.; Chernikova, E. V. *Polymers*, **14**, 555 (2022).
13. Al-Harthi, M.; Khan, M. J.; Abbasi, S. H.; Soares, J. B. P. Gradient Copolymers by ATRP in Semibatch Reactors: Dynamic Monte Carlo Simulation. *Macromol. React. Eng.*, **2009**, *3*, 148–159.
14. Moskowitz, J. D.; Wiggins, J. S. Semibatch RAFT copolymerization of acrylonitrile and Nisopropylacrylamide: Effect of comonomer distribution on cyclization and thermal stability. *Polymer*, **2016**, *84*, 311–318.
15. Toms, R. V.; Balashov, M. S.; Shaova, A. A.; Gerval'd, A. Yu.; Prokopov, N. I.; Plutalova, A. V.; Grebenkina, N. A.; Chernikova, E. V. Copolymers of Acrylonitrile and Acrylic Acid: Effect of Composition and Distribution of Chain Units on the Thermal Behavior of Copolymers. *Polym. Sci., Ser. B.*, **2020**, *62* (2), 102–115.
16. Toms, R. V.; Balashov, M. S.; Gerval'd, A. Yu.; Prokopov, N. I.; Plutalova, A. V.; Berkovich, A. K.; Chernikova, E. V. Influence of Synthesis Method on the Properties of Carbon Fiber Precursors Based on Acrylonitrile and Acrylic Acid Copolymers. *Polym. Sci., Ser. B.*, **2020**, *62* (6), 447–457.
17. Bahrami, S.H.; Bajaj, P.; Sen, K. Thermal Behavior of Acrylonitrile Carboxylic Acid Copolymers. *J. Appl. Polymer Sci.*, **2003**, *88* (3), 685–698.
18. Devasia, R.; Nair, C. P. R.; Sivadasan, P.; Katherine, B. K.; Ninan, K. N. Cyclization reaction in poly(acrylonitrile/itaconic acid) copolymer: An isothermal differential scanning calorimetry kinetic study. *J. Appl. Polymer Sci.*, **2003**, *88* (4), 915–920.
19. Sivy, G. T.; Coleman, M. M. Fourier transform IR studies of the degradation of polyacrylonitrile copolymers—II: Acrylonitrile/methacrylic acid copolymers. *Carbon*, **1981**, *19* (2), 127–131.
20. Coleman, M. M.; Sivy, G. T. Fourier transform ir studies of the degradation of polyacrylonitrile copolymers—I: Introduction and comparative rates of the degradation of three copolymers below 200°c and under reduced pressure. *Carbon*, **1981**, *19* (2), 123–126.
21. Sivy, G. T.; Coleman, M. M. Fourier transform IR studies of the degradation of polyacrylonitrile copolymers—IV: Acrylonitrile/acrylamide copolymers. *Carbon*, **1981**, *19* (2), 137–139.

22. Coleman, M.M.; Sivy, G.T.; Painter, P.C.; Snyder, R.W.; Gordon, B. III. Studies of the degradation of acrylonitrile/acrylamide copolymers as a function of composition and temperature. *Carbon*, **1983**, *21* (3), 255–267.
23. Sivy, G.T.; Gordon, B. III; Coleman, M.M. Carbon, Studies of the degradation of copolymers of acrylonitrile and acrylamide in air at 200 °C. Speculations of the role of the preoxidation step in carbon fiber formation. *Carbon*, **1983**, *21* (6), 573 – 578.
24. Takahashi, A.; Tanaka, H.; Kagawa, I. The Analysis and Solubility of Acrylonitrile-Acrylamide Copolymers. *Kogyo Kagaku Zasshi*, **1967**, *70*, 988–992.
25. Chapiro, A.; Perec-Spitzer, L. Influence des solvants sur la copolymerisation de l'acrylamide avec l'acrylonitrile. *Eur. Polym. J.*, **1975**, *11*, 59 – 69.
26. Hou, C.; Ying, L.; Wang, C. Determination of monomer apparent reactivity ratios for acrylonitrile-acrylamide copolymerization system. *J. Mater. Sci.*, **2005**, *40*, 609 – 612.
27. Sun, J.; Wang, K.; Wang, J.; Qin, C.; Dai, L. Pre-oxidation nanofibers from acrylonitrile-acrylamide copolymers synthesized by solvent-water polymerization. *Adv. Mater. Res.*, **2011**, *175-176*, 164–169.
28. Cheng, R.; Zhou, Y.; Wang, J.; Cheng, Y.; Ryu, S.; Jin, R. High Char-Yield in AN-AM Copolymer by Acidic Hydrolysis of Homopolyacrylonitrile. *Carbon Lett.*, **2013**, *14* (1), 34–39.
29. Han, N.; Zhang, X.-X.; Wang, X.-C. Various Comonomers in Acrylonitrile Based Copolymers: Effects on Thermal Behaviour. *Iran. Polym. J.*, **2010**, *19* (4), 243–253.
30. Chernikova, E.V.; Kishilov, S.M.; Plutalova, A.V.; Kostina, Yu.V.; Bondarenko, G.N.; Baskakov, A.A.; Il'in, S.O.; Nikolaev, A.Yu. Specific Features of the Copolymerization of Acrylonitrile and Acrylamide in the Presence of Low-Molecular-Mass and Polymeric Trithiocarbonates and Properties of the Obtained Copolymers. *Polym. Sci., Ser. B.*, **2014**, *56* (5), 553 – 565.
31. Maksimov, N. M.; Toms, R. V.; Balashov, M. S.; Gerval'd, A. Yu.; Prokopov, N. I.; Plutalova, A. V.; Kuzin, M. S.; Skvortsov, I. Yu.; Kulichikhin, V. G.; Chernikova, E. V. Novel Potential Precursor of Carbon Fiber Based on Copolymers of Acrylonitrile, Acrylamide, and Alkyl Acrylates. Polym. Sci., Ser. B., **2014**, *64* (5), 670 – 687.
32. Chernikova, E. V.; Terpugova, P. S.; Garina, E. S.; Golubev, V. B. Controlled radical polymerization of styrene and n -butyl acrylate mediated by trithiocarbonates. *Polym Sci Ser A*, **2007**, *49* (2), 108-119.
33. *Polymer Handbook*, Brandrup, J., Immergut, E. H., Grulke, E. A., Eds.; Wiley: New York, USA, 1999.
34. Holland-moritz, K.; Siesler, H. W. Infrared Spectroscopy of Polymers. Appl. Spectrosc. Rev., **1976**, *11* (1), 1–55.
35. Kissinger, H.E. Reaction Kinetics in Differential Thermal Analysis. *Anal. Chem*. 1957, 29(11), 1702-1706.
36. Collins, G.L.; Thomas, N.W.; Williams, G.E. Kinetic relationships between heat generation and nitrile consumption in the reaction of poly(acrylonitrile) in air at 265°C. *Carbon*, **1988**, *26* (5), 671-679.
37. Ouyang, Q.; Cheng, L.; Wang, H.; Li, K. Mechanism and kinetics of the stabilization reactions of itaconic acid-modified polyacrylonitrile. *Polym. Degrad. Stab.*, **2008**, *93* (8), 1415-1421.
38. *RAFT Polymerization: Methods, Synthesis, Applications*; Moad, G., Rizzardo, E., Eds.; Wiley-VCH: Weinheim, Germany, 2022.
39. *Handbook of RAFT Polymerization*, Barner-Kowollik C., Ed.; Wiley: Weinheim, Germany, 2008.
40. Moad, G.; Rizzardo, E.; Thang, S. H. Living Radical Polymerization by the RAFT process – A Third Update. *Aust. J. Chem.*, **2012**, *65*, 985–1076.
41. Moad, G. Mechanism and Kinetics of Dithiobenzoate-Mediated RAFT Polymerization – Status of the Dilemma. *Macromol. Chem. Phys.*, **2014**, *215*, 9–26.
42. Van Doremaele, G.H.J.; German, A.L.; de Vries, N.K.; van der Velden, G.P.M. ^{1}H and ^{13}C NMR investigation of the intramolecular structure of solution and emulsion styrene-methyl acrylate copolymers. *Macromolecules*, **1990**, *23*, 4206-4215.
43. Chernikova, E.V.; Sivtsov, E.V. Reversible Addition-Fragmentation Chain-Transfer Polymerization: Fundamentals and Use in Practice. *Polym. Sci., Ser. B.*, **2017**, *59* (2), 117 – 146.
44. Wu, X.; Zhang, X.; Lu, C.; Ling, L. Thermo-chemical reactions and structural evolution of acrylamide-modified polyacrylonitrile. *Chin. J. Polym. Sci.*, **2010**, *28* (3), 367–376.